

ARIES imaging polarimeter

B. S. Rautela, G. C. Joshi, J. C. Pandey*

Aryabhata Research Institute of Observational Sciences, Naini Tal - 263 129, India

Received 30 March 2004; accepted 9 August 2004

Abstract. An Imaging Polarimeter has been fabricated for use with liquid-N₂ cooled CCD camera and is designed to suit 104-cm Sampurnanand telescope with an f/13 focus at Aryabhata Research Institute of Observational Sciences (ARIES), Naini Tal. The instrument measures the linear polarisation in broad B, V and R band and has a field of view $\sim 2' \times 2'$. We are presenting here some observations regarding the polarisation of some polarised as well as unpolarised stars with a view to show the performance of our polarimeter.

Keywords : polarimeter – polarization

1. Introduction

Realizing the immense potential of polarization measurements in the study of astronomical objects and taking the advantage of two dimensional array and taking view of the fact that ARIES, Nainital does not have one and acquiring a ready-made polarimeter would cost a lot, we decided to fabricate a polarimeter on the lines of IMPOL by Ramaprakash et. al. 1998 (hereafter IUIMPOL) which has come up on the principle given by (Sen & Tandon 1994), which again has taken into consideration the ideas suggested by the various authors (Ohman 1939; Appenzeller 1967 etc). These ideas have been emerged out, mainly taking into considerations the advantages of aperture polarimetry as against imaging polarimetry.

*E-mail: jeewan@upso.ernet.in

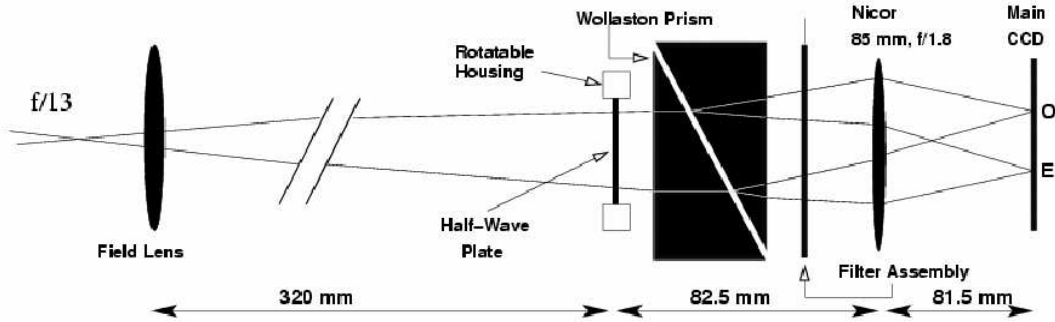


Figure 1. Optical Layout of IMPOL.

2. The Instrument

We have plans to use the polarimeter as a back-end instrument for 104-cm Sampurnanand f/13 Cassegrain telescope. Our polarimeter is different from that of IUIMPOL in the sense that we are using a ST4 mounted on a 8 inch finder telescope of the main telescope instead of a built in guidance unit as in the case with IUIMPOL (Fig. 1). The block diagram of the control system has been shown in Fig. 2. As illustrated in Fig. 1, a f/13 beam from the telescope falls on the field lens (50mm, f/6 Karl Lambrecht part no. 322305) which in combination with the camera lens (85mm, f/1.8) makes the image of the object at the CCD chip. In between the camera lens and the field lens are mounted a rotatable half-wave plate (HWP) and a Wollaston prism. The rotatable HWP gives components of electric vector polarised orthogonally of varying intensities after emerging out of the Wollaston prism as an analyser. The axis of the Wollaston prism is aligned to north - south axis of the telescope and the HWP is placed in such a way that the fast axis of the plate is aligned to the axis of the prism. Fast axis of the plate and axis of the prism are kept normal to the optical axis of the system. At an angle α of the HWP we measure the intensities of the two orthogonally polarised beams. Now when we rotate the HWP by an angle α , the electric vector rotates through an angle 2α . A ratio $R(\alpha)$ has been defined in such a way that:

$$R(\alpha) = \frac{I_e/I_o - 1}{I_e/I_o + 1} = p \cos(2\theta - 4\alpha) \quad (1)$$

where, I_e = Intensity of extra-ordinary image.

I_o = Intensity of ordinary image.

p = fraction of the total light in the linearly polarised condition.

θ = polarising angle which is the direction of the electric vector with respect to north-south direction.

α = angle which the HWP makes with the NS direction.

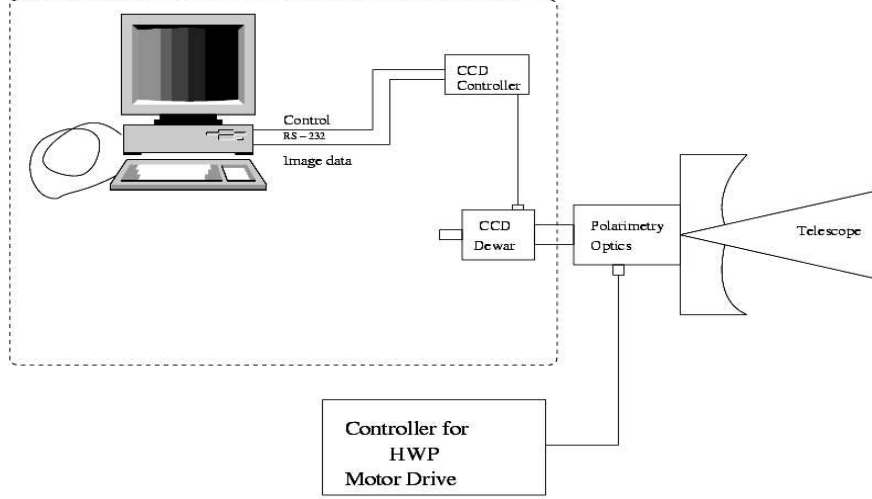


Figure 2. Polarimeter control system.

The values at 0^0 and 22.5^0 directly measure the normalised stokes parameter q ($=Q/I$) and u ($=U/I$). The linear polarisation (p) and position angle of the polarisation vector (θ) is given by

$$p = \sqrt{q^2 + u^2} \quad \text{and} \quad \theta = 0.5\arctan(q/u)$$

Additional two values are measured at $\alpha = 45^0$ and 67.5^0 due to non-responsivity of the system (see the section 4)

The detector is a TK 1KX1K CCD camera cooled by liquid-N₂ (see Table 1 for details). For each object within a field of view, two images (ordinary and extra-ordinary) formed are separated by 15 pixels in CCD frame. In case of overlap of the ordinary and extra-ordinary images, we are aiming to place a grid of parallel obscuring strips at focal plane of the telescope. We have checked whether CCD has a uniform response over the entire frame. Further, simultaneous measurements of two orthogonal components take care of the atmospheric effect. All the components have anti reflection coating to minimize the polarization due to reflection and the inside of the polarimeter has been painted black to avoid stray light. We find that some of the components have got their anti reflection coating slightly damaged which may cause some polarization due to reflection. The uncertainty (σ_α) in the position of HWP give a maximum uncertainty in polarisation

Table 1. The parameters of CCD camera

Parameters	Value
CCD chip size	1024 × 1024 pixel ²
Pixel size	24μ × 24μ
Active field of view	2' × 2'
Quantum efficiency	B(17 %) V(20 %) R(35 %)
Regulated Temperature	-110 ^o
Readout speed	40 KHz
Read noise	7.0 e ⁻
Gain	11.98 e ⁻ /ADU
Dark Current	< 5 -10 e ⁻ /pixel/sec

$\sigma_p = p * \sigma_\alpha$ (Serkowski 1974), where α is expressed in radians. An uncertainty of 0.1 degree in position of HWP (a typical value if rotated by steeper motor) will give $\sigma_p = 0.002p\%$. The instrument measures linear polarization in the wavelength region 400-800nm.

3. Performance estimates

The typical observing conditions for our imaging polarimeter are:

Background sky = 22.5 mag arsec⁻² at V band

plate scale = 15 arcsec mm⁻¹ (f/13 beam of 104-cm telescope)

light collecting area of the telescope = 1.08 × 10⁴ cm²

software aperture for photometry = ~ 40 arcsec²

For small value of p the number of photoelectrons corresponding to ordinary and extra-ordinary images are approximately equal. So the error in the measurement of p and θ due to photon noise are given by (Ramaprakash 1998)

$$\sigma_p = \frac{\sqrt{(N + N_b)}}{N} \times 100\% \quad \text{and} \quad \sigma_\theta = 0.5 \times \frac{\sigma_p}{p} \text{ rad} \quad (2)$$

where N and N_b are number of photoelectrons corresponding to the source and background. For the star of the apparent visual magnitude $m_v = 13$ the value of σ_p is ~ 0.18% with an exposure time of 2.0 minute. Fig. 3 shows plot between visual magnitude and the theoretically estimated error in the measurements of the polarisation, due to photon statistics alone. Actual measured error is also plotted against the visual magnitude in the same figure. In Fig. 3 solid circles and triangles represent the theoretically estimated error and the actual measured error, respectively.

4. Observations and Data reductions

Observations have been made at ARIES using 104-cm telescope. All the measurements were taken in the white/V light for testing our instrument. Three to four CCD frames

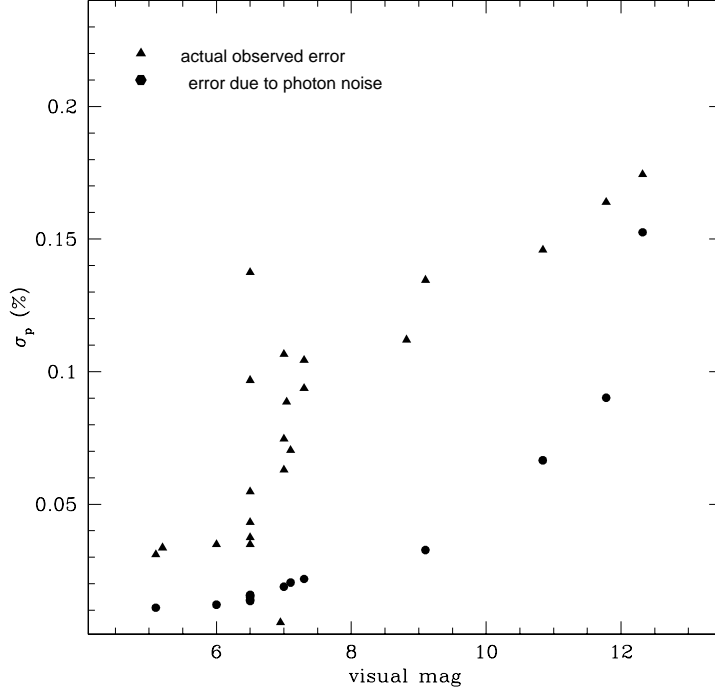


Figure 3. Plot of σ_p versus visual magnitude. Solid circle represents theoretically estimated error due to photon noise and triangle represents the actual error obtained.

of same exposure time at each position of the HWP have been taken for each object. The exposure time is ranging from 1 to 120 secs depending on the source magnitude. Number of bias and twilight flat frames were also taken during the observing run. We have observed 9 polarised stars, as given in Table 2. Unpolarised standards were also taken to check the instrumental polarization.

IRAF¹ was used for the data reduction. Bias was subtracted from target image and then divided the resulting image by normalised bias subtracted flat field image. After that cosmic hits were removed using the *crutil* package in IRAF. A *daofind* task under *apphot* package finds the center of the star. Then through the *phot* task we have determined the flux of ordinary and extra-ordinary images.

Even after the flat fielding the responsivity of the CCD frame to the two orthogonal images may not be same and may be a function of its surface. So the actual flux ratio

¹IRAF is distributed by the National Optical Astronomy Observatories, USA

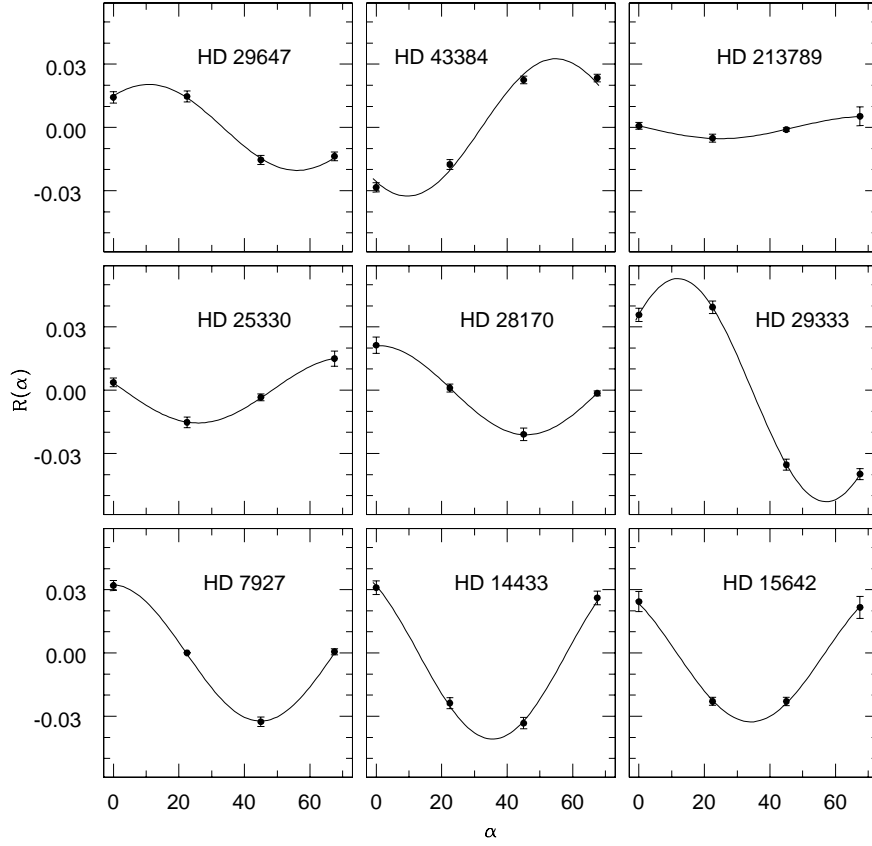


Figure 4. The best cosine fit for the 4 values of $R(\alpha)$ for different stars. The star name is mentioned inside each panel.

may differ from observed one and related by the following formula (Ramaprakash 1998)

$$\frac{I_e(\alpha)}{I_o(\alpha)} = \frac{F_o}{F_e} \times \frac{I'_e(\alpha)}{I'_o(\alpha)} \quad (3)$$

where

$$\frac{F_o}{F_e} = \left[\frac{I'_o(0^0)}{I'_e(45^0)} \times \frac{I'_o(45^0)}{I'_e(0^0)} \times \frac{I'_o(22.5^0)}{I'_e(67.5^0)} \times \frac{I'_o(67.5^0)}{I'_e(22.5^0)} \right]^{1/4}$$

and $I'_e(\alpha)$ and $I'_o(\alpha)$ are actual measured flux.

To get the best values of p and θ we have fitted eq. (1) to the four values of $R(\alpha)$

determined using eq. (1) and (3) by linear least square deviation method. Fig. 4 shows the best fit of these four points for the stars mentioned in Table 2.

5. Results

This section describes the performance of our instrument. We have measured the polarisation of 9 standard polarised stars. Table 2 shows our measured p and θ in V band along with the standard values.

Table 2. Polarised stars. a - Heiles 2000, b - Whittet, et al. 2001 and c - Ramaprakash, et al. 1998.

Object	V (mag)	Our measured values		Standard Values		Ref.
		$p(\%)$	$\theta(\text{degree})$	$p(\%)$	$\theta(\text{degree})$	
HD 7927	5.0	3.23 ± 0.03	90.0 ± 0.8	3.23 ± 0.20	94.0 ± 0.5	a
HD 14433	6.4	4.08 ± 0.12	109.4 ± 0.8	3.87 ± 0.20	112.0 ± 1.5	a
HD 15642	8.5	3.26 ± 0.12	112.0 ± 0.6	3.13 ± 0.20	115.0 ± 1.8	a
HD 25330	5.7	1.55 ± 0.02	128.7 ± 0.4	1.52 ± 0.03	134.4 ± 0.7	a
HD 28170	8.9	2.11 ± 0.02	88.8 ± 0.2	2.03 ± 0.03	89.4 ± 0.7	a
HD 29333	8.5	5.29 ± 0.01	66.1 ± 0.1	5.25 ± 0.02	70.9 ± 1.5	b
HD 29647	8.4	2.10 ± 0.01	66.5 ± 0.1	2.30 ± 0.02	71.4 ± 7.3	b
HD 43384	6.3	3.08 ± 0.08	161.4 ± 2.3	3.05 ± 0.04	170.6 ± 1.3	c
HD 213789	5.9	0.53 ± 0.01	130.7 ± 0.5	0.53 ± 0.04	133.7 ± 1.9	d

Number of unpolarised star (see Table 3) were also observed to check the polarisation by the instrument. Fig. 5 show the plot of $q = R(0^\circ)$ against $u = R(22.5^\circ)$ for unpolarised standards in white light. The low correlation ($r = 0.103$) with probability of no correlation

Table 3. Unpolarised stars.

Object	V(mag)	$q(\%)$	$u(\%)$	Object	V(mag)	$q(\%)$	$u(\%)$
HD 21447	5.10	0.011	0.029	HD 10476	5.20	0.027	-0.020
HD 100623	6.00	0.022	0.027	HD 102438	6.50	0.026	-0.027
HD 125184	6.50	0.043	0.004	HD 42807	6.50	-0.051	-0.020
HD 42807	6.50	0.096	0.012	HD 90508	6.50	0.128	0.050
HD 103095	6.50	0.031	0.016	HD 90156	6.95	0.005	-0.002
HD 9540	7.00	0.059	0.022	HD 65583	7.00	0.063	-0.086
HD 97343	7.04	-0.025	0.085	HD 65583	7.00	0.033	0.067
HD 144287	7.10	0.068	0.018	HD 98281	7.30	0.067	0.080
HD 98281	7.30	-0.090	-0.026	HD 109055	8.82	0.068	0.089
HD 94851	9.10	0.073	-0.113	BD +33 2642	10.842	0.041	0.140
G 191B2B	11.78	-0.017	0.163				

55 % indicate low instrumental polarisation. The average value of q (= 0.032%) and u (= 0.024%) gives the value of instrumental polarisation $\sim 0.040\%$.

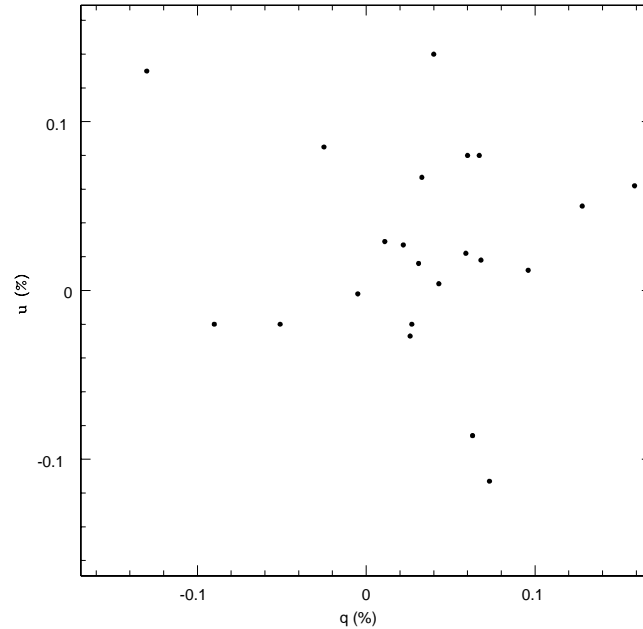


Figure 5. Plot of q vs u .

Acknowledgment

We are thankful to various sections, namely the electronics shop, the mechanical workshop and the optics shop for their help at various stages of the development of the instrument. We thank to Prof. Ram Sagar for his useful discussion during the development of the instrument. We are also thankful to an anonymous referee for the useful comments and suggestions.

References

- Appenzeller I. 1967, *PASP*, **79**, 136.
 Heiles Carl, 2000, *AJ*, **119**, 923.
 Ohman Y. 1939, *MNRAS*, **99**, 624.
 Ramaprakash A. N., et al., 1998, *A&A*, **128**, 369.
 Sen A. K., Tandon S. N., 1994, in *Instrumentation in Astronomy VIII*, Ed. D. L. Crawford, SPIE proceedings, **Vol. 2198**, part 1, P. 264.

- Serkowski K., 1974, “*Polarimetric techniques*”, *Methods of Exp. Phys.: Astrophysics*, ed. M Carleton, **Vol-12 Part A**, pp. 361 - 414.
- Whittet D. C. B., et al., 2001, *ApJ*, **547**, 872.